RSC Advances

PAPER

View Article Online
View Journal | View Issue

Cite this: *RSC Adv.*, 2014, **4**, 25940

Structural optimization of super-gelators derived from naturally-occurring mannose and their morphological diversity†

Fumiyasu Ono,*[a] Hisayuki Watanabe[ab] and Seiji Shinkai[c]

Received 3rd February 2014
Accepted 28th April 2014

DOI: 10.1039/c4ra03096f

www.rsc.org/advances

Mannose derivatives were synthesized as low molecular-weight gelators with various alkoxy substituents on the aromatic ring of methyl-4,6-*O*-benzilidene-α-D-mannopyranoside . Most of these mannose derivatives could gel in various solvents, such as octane, cyclohexane, toluene, ethylene glycol and ethanol solutions, at concentrations lower than 2.0 wt%. In particular, the critical gelation concentration (CGC) of methyl-4,6-*O*-(4-butoxybenzylidene)-α-D-mannopyranoside (**2**) for squalane was only 0.025 wt%, one of the lowest CGCs we have ever experienced. The observations of xerogels by FE-SEM, TEM and AFM revealed that the length of the alkoxy chains of the mannose derivatives influences the gel morphologies. Moreover, the toluene gels formed from the mannose derivatives **1–6** functionalized by a linear alkoxy group exhibited thixotropic properties. Interestingly, the gels of various solvents formed from methyl-4,6-*O*-(4-dodecyloxybenzylidene)-α-D-mannopyranoside (**6**) (with the longest alkoxy chain on the aromatic ring in this paper) exhibited thixotropic properties. Thus, we confirmed that alkoxy groups on the aromatic ring exert noticeable effects on the gelation properties of these mannose derivatives.

Introduction

Gelators are materials capable of forming a gel structure, which can contain fluid in its three-dimensional network. Specifically, a hydrogel accommodates water, whereas an oil gel or an organogel accommodates oil or organic solvent, respectively. Polymeric gels supported by a cross-linked three-dimensional network have been a primary class of studied gelator compounds. Recently, there has been a marked increase in studies on low molecular-weight gelators (LMWGs) that are constructed from self-assemblies of low molecular-weight compounds. Because of the synthetic ease and the diversity of self-assemblies, one can integrate various additional functions within the LMW supramolecular gels. These advantages are characteristics of LMWGs that are not available with polymeric gels. The development of LMWGs has proceeded with both aqueous and organic solvents.[1–12] One can expect that the continuing endeavour to develop LMWGs will eventually result in their implementation in industrial, cosmetic, electronic, optical device, oil spill and medicinal applications.

A variety of the physical properties inherent to LMWGs can be applied to integrate unique functions within the gels. One of the most fundamental properties is the phase transition between the sol phase and the gel phase, which can be used as a stimulus to control the imparted functions. It is possible to induce phase transition by heat, mechanical means, light, *etc.* In 1998, Shinkai's group reported that sugars are useful as basic skeletons to design LMWGs, where the gels are stabilized owing to the hydrogen-bonding interactions among the OH groups.[13] As sugars are naturally-occurring materials, one can expect to apply them to those purposes that require environmentally-friendly properties and functions.[14–19] For example, Jadhav *et al.* prepared gels using sorbitol or mannitol derivatives, which can selectively remove oil from an oil–water mixture,[15] whereas Vidyasagar *et al.* reported that mannitol derivatives can form transparent self-standing oil gels applicable to film processing.[17]

We previously reported the gelation ability of methyl-4,6-*O*-benzilidene-α-D-mannopyranoside (referred to as '**Bn**' in this paper).[13,20–23] It was found that this mannose derivative can form gels accommodating various solvents: in particular, the ability to gelate both water and certain organic solvents is unique.[13,20–36] However, the gels formed from this mannose skeleton could be either clear or slightly opaque (*e.g.*, the toluene-loaded gel was slightly opaque; Fig. 1, left). We have newly synthesized a mannose derivative functionalized with a methoxy group at the *para* position of the aromatic ring and evaluated its gelation ability for toluene. Interestingly, using this derivative resulted in a transparent toluene-loaded gel

[a]*Advanced Materials Research Laboratory, Collaborative Research Division, Art, Science and Technology Center for Cooperative Research, Kyushu University, 4-1, Kyudai-Shinmachi, Nishi-ku, Fukuoka, Fukuoka 819-0388, Japan*

[b]*Nissan Chemical Industries, Ltd., 10-1 Tsuboi-Nishi 2-chome, Funabashi, Chiba 274-8507, Japan*

[c]*Institute of Systems, Information Technologies and Nanotechnologies (ISIT), 4-1 Kyudai-Shinmachi, Nishi-ku, Fukuoka, Fukuoka 819-0388, Japan*

† Electronic supplementary information (ESI) available. See DOI: 10.1039/c4ra03096f

Fig. 1 Images of toluene-filled gel formed from methyl-4,6-*O*-benzylidene-α-D-mannopyranoside (**Bn**) in a previous work (left) and **1** (right).

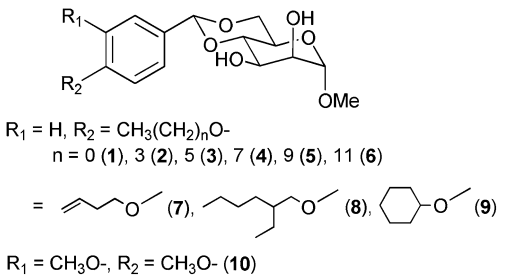

Fig. 2 Structures of the mannose derivatives investigated in this study.

showing thixotropic behaviour (Fig. 1, right). The finding implies that the slight modification of the gelator's structure greatly changes the gelation ability.

Stimulated by this finding, we extensively studied the possible correlation between the structures of mannose derivatives as LMWGs and their physical gelation properties, such as critical gelation concentration, gel–sol phase transition temperature, thixotropy, *etc.* Specifically, we investigated the influence of the structures of the alkoxy groups, such as linear *versus* branched, saturated *versus* unsaturated, and *para*-substituted *versus meta*-substituted on the aromatic ring, *etc.* (Fig. 2).

Results and discussion

Synthesis of mannose-based gelators

The mannose derivatives used as LMWGs were synthesized from the corresponding aromatic aldehydes in two steps (Fig. 3). Several *O*-substituted aromatic aldehydes were synthesized from 4-hydroxybenzaldehyde and the corresponding alkylbromides using K_2CO_3 as a base in DMF at 80 °C or 150 °C. The acetals (mannose derivative precursors) were synthesized by the reaction of the corresponding aldehydes and trimethyl

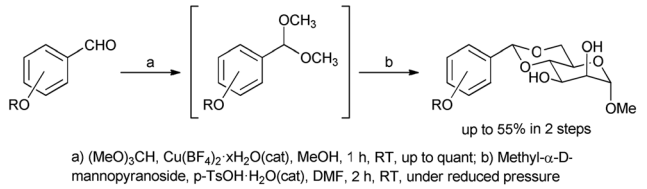

Fig. 3 Synthetic scheme of the mannose-based gelators.

orthoformate in the presence of a $Cu(BF_4)_2$ catalyst in methanol at room temperature (RT). The final acetal compounds were derived by the reaction of aldehydes and methyl-α-D-mannopyranoside, the reaction being catalysed by *p*-TsOH in DMF at RT under reduced pressure. The yields in this reaction were up to 55%. These products were characterized by ^{1}H NMR, ^{13}C NMR and HRMS.

Gelation abilities

The gelation abilities of the mannose-based derivatives were determined for a range of 19 different solvents and 6 aqueous mixtures; in each case, 2.0–20 mg of mannose derivative was submerged in 1.0–8.0 mL of the desired solvent in a sealed vial while being heated (Table 1). The sample vial was cooled to RT, then the sample vial was inverted after 1 h. We classified the obtained results as follows: a transparent gel, a translucent gel, an opaque gel, a precipitate and a clear solution or a suspension. The results are summarized in Table 1.

The abbreviations used for each mannose derivative are as follows: linear alkoxy groups, **1–6**; linear alkoxy group with a terminal olefin, **7**; branched alkoxy group at the *para* position on the aromatic ring, **8**; cyclic alkoxy group *para*-substituted on the aromatic ring, **9**; and methoxy group at the *meta* and *para* positions on the aromatic ring, **10**. Derivatives **1–8** served as gelators for linear and cyclic alkanes (octane, cyclohexane, squalane and squalene), an aromatic solvent (toluene) and decamethylcyclopentasiloxane (DOW CORNING TORAY SH 245 FLUID, referred to as 'SH245' in this paper). Surprisingly, the critical gelation concentration (CGC) of **2** for squalane was 0.025 wt%, one of the lowest CGCs we have ever experienced. In other words, this gel consisted of 99.975 wt% squalane. In addition, **1–6** and **7** were able to gelate olive oil, isopropyl myristate (IPM) and even ethylene glycol (in spite of the protic solvent). Both **2** and **7** gelated water. On the other hand, **9** and **10** exhibited no gelation ability for any of these solvents.

As demonstrated in Fig. 4, an inverse correlation of CGC and solvent polarity was demonstrated with six analogous gelators. We estimated the CGCs of **2** and **6** to be 0.5 wt% (14.1 mM) and 2.0 wt% (42.9 mM) in toluene, respectively. In contrast, the CGCs of **2** and **6** were estimated to be 2.0 wt% (56.4 mM) and 0.25 wt% (5.4 mM), respectively, in ethylene glycol. These apparently anomalous tendencies are rationalized in terms of the inversion of the aggregation modes of nonpolar solvents and polar solvents: that is, in toluene, the sugar moiety should occupy the core and the alkoxy group should cover the shell surface, whereas the core–shell relationship should be inverted. The gelation abilities of the mannose derivatives in DMSO–H_2O

Table 1 The observed critical gelation concentration (CGC) values (wt%) and qualitative note[a] (qual. only if CGC could not be determined, and CGC values only if the gel was transparent)

Entry	Solvent	1	2	3	4	5	6	7	8	9	10
1	Octane	0.1	0.05	0.1	0.1	0.1	0.25	0.1 PG	0.05	IS	IS
2	Cyclohexane	0.25	0.05	0.05	0.1	0.1	0.1	0.1	0.25	IS	IS
3	Squalane	0.05	0.025[c]	0.05	0.05	0.05	0.1	0.05	0.1	IS	IS
4	Squalene	0.1	0.05	0.1	0.25	0.25	0.25	0.1	0.25	P	P
5	Toluene	0.5	0.5	1.0	1.0	2.0	2.0	0.5	S	IS	IS
6	SH245	0.05	0.05	0.05	0.1	0.25	0.5	0.05	0.1	IS	IS
7	Olive oil	0.5	0.5	1.0	1.0	1.0	1.0	0.5	S	IS	P
8	IPM	0.5	0.5	1.0	1.0	1.0	1.0	0.5	S	IS	IS
9	Chloroform	S	S	S	S	S	S	S	S	S	S
10	Ethyl acetate	S	S	S	S	S	S	S	S	S	S
11	Acetone	S	S	S	S	S	S	S	S	S	S
12	Cyclohexanone	S	S	S	S	S	S	S	S	S	S
13	Acetonitrile	S	S	S	S	S	S	S	S	P	S
14	DMSO	S	S	S	S	S	S	S	S	S	S
15	EtOH	S	S	S	S	S	S	S	S	S	S
16	MeOH	S	S	S	S	S	S	S	S	S	S
17	Ethylene glycol	S	2.0 OG	2.0 TL	1.0 TL	0.5 TL	0.25 TL	S	P	S	S
18	Glycerol	S	2.0 TL	P	P	P	P	P	P	P	S
19	Water	P	0.1 OG	P	IS	IS	IS	0.1 TL	IS	IS	P
20	DMSO–H_2O (75/25)[b]	S	S	2.0 OG	1.0	0.5 TL	0.5 TL	S	S	S	S
21	DMSO–H_2O (50/50)[b]	S	0.5 TL	0.1 TL	0.05	0.1 TL	0.25 TL	1.0 OG	P	P	S
22	DMSO–H_2O (25/75)[b]	S	0.1 TL	0.1 TL	0.25 TL	P	P	0.25 TL	IS	IS	S
23	EtOH–H_2O (75/25)[b]	S	S	S	S	2.0 OG	2.0 OG	S	S	S	S
24	EtOH–H_2O (50/50)[b]	S	1.0 OG	0.5 OG	0.5 OG	0.25 OG	0.25 TL	2.0	P	S	S
25	EtOH–H_2O (25/75)[b]	P	0.1 TL	0.1 TL	0.05 TL	P	P	0.25 OG	IS	IS	S

[a] TL, translucent gel; OG, opaque gel; S, solution; IS, insoluble; P, precipitation; PG, partial gel. [b] Numbers in parentheses are the ratios of the mixed solutions (vol/vol). [c] After 12 h.

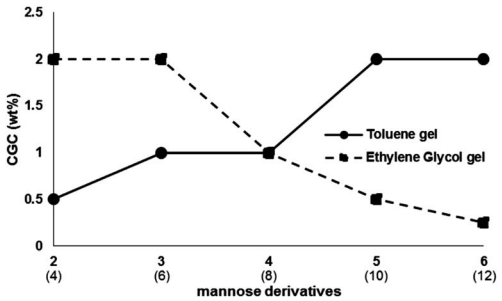

Fig. 4 The CGCs of mannose derivatives **2–6**, in toluene and ethylene glycol (the numbers in parentheses are the lengths of the alkoxy chains).

and EtOH–H_2O mixtures were also investigated using derivatives **1–6** and **7**. As demonstrated in Fig. 5, the higher water-content mixtures are gelated more easily with shortening of the lengths of the linear alkoxy chains.

Gel–sol phase transitions

In Fig. 6, the gel–sol phase transition temperatures (T_{gel}) of **Bn**, **1–6** and **7** in toluene are plotted against the gelator concentrations in order to compare their concentration-dependent gelation properties. When compared at the same concentration, the T_{gel} values always maintained the following order from the highest to the lowest: **7**, **1**, **2**, **Bn**, **3**, **4**, **5**, **6**. The T_{gel} values of **7**, **1** and **2** were higher than that of **Bn** without alkoxyl group functionalization on the aromatic ring. Additionally, since the T_{gel} of **7** was consistently higher than those of the other mannose derivatives, the thermal stabilization of toluene gel is likely due to the π–π interaction occasionally observed between terminal olefins.[37]

Morphology of xerogels

We investigated the morphologies of several organogels prepared from **2** and **6** with toluene, cyclohexane and a 50/50 (vol/vol) mixture of ethanol and a few hydrogels, using field

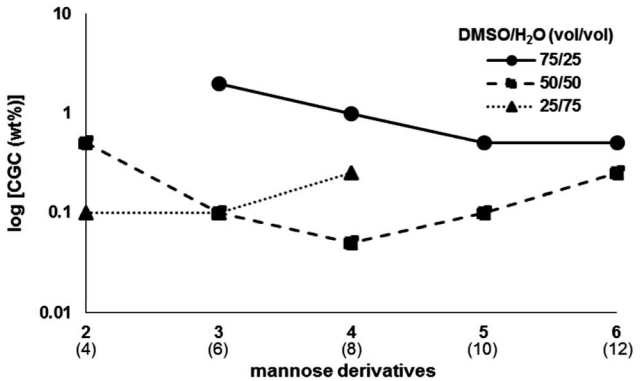

Fig. 5 The CGCs of mannose derivatives **2–6**, in DMSO–H_2O mixtures (the numbers in parentheses are the lengths of the alkoxy chains).

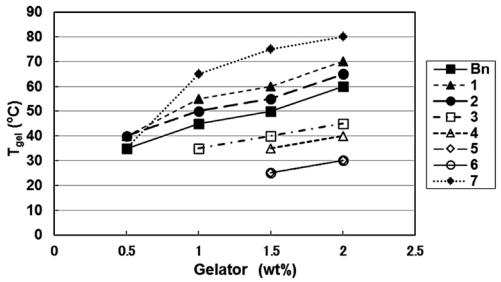

Fig. 6 T_{gel} *vs.* gelator concentration in toluene.

emission scanning electron microscopy (FE-SEM), transmission electron microscopy (TEM) and atomic force microscopy (AFM) (Fig. 7). For the FE-SEM measurements, the xerogels were obtained by freezing and pumping the gel for 5–14 h. For the TEM measurements, the samples were obtained by dipping a carbon-coated copper grid into the gel and negatively staining it with 1% phosphotungstic acid (adjusted to pH 7). For the AFM measurements, a droplet of a toluene solution containing **2** or **6** at 0.02 wt% below the CGC value was placed on highly-ordered pyrolytic graphite (HOPG). After 1 h, the substrates were dried under vacuum for more than 12 h.

The FE-SEM image of the xerogel prepared from **2** and cyclohexane displayed a three-dimensional entangled fibrous network 10–20 nm in width, whereas that of **6** displayed a sheet-like structure. The FE-SEM images of the xerogels formed from both **2** and **6** with toluene displayed sheet-like structures. For the TEM images of gels prepared with toluene, **2** displayed a fibrous network 140–200 nm in width, whereas **6** displayed a flowing stream-like structure. Interestingly, the AFM image of the dried sample for a toluene solution of **2** at 0.02 wt% below the CGC value also depicted the fibrous networks when observed by TEM. Similarly, the AFM image of **6** in toluene showed the flowing stream-like structure. These phenomena reveal that the rates of the self-assembly processes involving mannose derivatives **2** and **6** are faster than the evaporation rate of toluene. In the previous work, the SEM image of the xerogel formed from **Bn** with toluene displayed the fibrous network,[19] whereas those of **2** and **6** displayed the sheet-like structures because of bundled fibers created by the van der Waals interactions between alkoxy chains. Furthermore, the difference in the TEM images obtained from **2** and **6** is attributable to the difference in the strength of the van der Waals interactions induced by the length of the alkoxy chains: that is, the TEM and FE-SEM images of the xerogels prepared from the cyclohexane gel and the toluene gel of **6** showed sheet-like and stream-like structures because of the stronger van der Waals interactions of **6**, which arises from having a longer alkoxy chain than **2**. For the xerogels prepared with the ethanol–water mixture, the FE-SEM image of **2** displayed both short and long, thick fibrous networks 130–180 nm in width, whereas that of **6** displayed right-handed helical fibrous structures 200–400 nm in width. These images were also observed for their corresponding TEM images. The FE-SEM and TEM images of the xerogel prepared from the hydrogel of **2** displayed both short and long, bundled

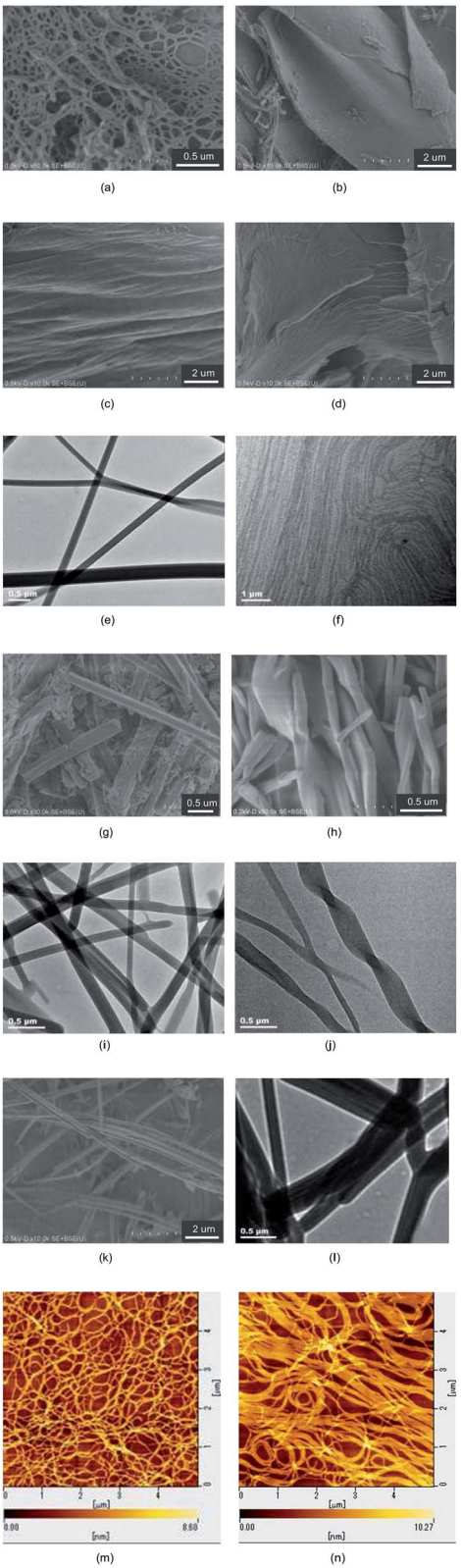

Fig. 7 FE-SEM images of xerogels: cyclohexane with (a) **2** and (b) **6**; toluene with (c) **2** and (d) **6**; EtOH–H_2O (50/50, vol/vol) with (g) **2** and (h) **6**; and (k) hydrogel of **2**. TEM images of gels as follows: toluene with (e) **2** and (f) **6**; EtOH–H_2O (50/50, vol/vol) with (i) **2** and (j) **6**; and (l) hydrogel of **2**. The AFM images of dried toluene solutions of (m) **2** and (n) **6** at 0.02 wt% on HOPG.

thick fibrous networks 150–550 nm in width. These characteristic xerogel morphologies prepared from the hydrogel of **2** are created by the periodic structure corresponding to the hexagonal organization, which is evidenced by XRD measurements described in the next section.

XRD measurements

The X-ray diffraction (XRD) patterns of the xerogels prepared from **2** and water show periodical reflection peaks (Fig. 8), which indicate that **2** indeed assembles into a hexagonal organization. The obtained long spacing distances (d) were 2.27 nm, 1.31 nm, 1.14 nm, 0.85 nm, 0.75 nm and 0.65 nm, which correspond to the ratios of 1 : 1, $\sqrt{3}$: 1, 2 : 1, $\sqrt{7}$: 1, 3 : 1 and $\sqrt{12}$: 1, respectively. The 2.27 nm length is shorter than twice that of the extended molecular length of **2** (1.78 nm by CPK molecular modelling) but longer than the length of one molecule. The aqueous gels prepared from **2**, therefore, should maintain an interdigitated bilayer structure with a thickness of 2.27 nm (Fig. 9). This value is compatible with a bilayer structure that has the alkoxy chain tilted with respect to a normal vector of the layer's plane. In addition, the wide-angle region of the X-ray diagram for the hydrogel of **2** revealed a series of sharp reflection peaks. This finding supports the view that the long alkoxy chain groups form the highly ordered interdigitated layer packing stabilized by hydrophobic interactions.

In contrast, the XRD diagram of the xerogel of **2** and toluene is remarkably different from that obtained in water; it has two broad peaks appearing at d = 4.26 and 2.03 nm in the small-angle region and one broad reflection peak in the wide-angle region. The main peak at 2.03 nm suggests an ordered arrangement of gelators in the fibrous structure. The weak peaks appearing at 4.26 and 0.62 nm are attributed to the bundled main fibers and the mannose moiety (self-organized by hydrogen bonding), respectively.

Next, we used XRD to measure the long spacing distances of **2**, **4** and **6** in the xerogels prepared from toluene (Fig. 10). The peaks appeared at 2.27 nm, 2.35 nm and 2.96 nm, respectively, indicating that the fiber diameter becomes thicker with an increase in the length of the alkoxy chain attached to the aromatic ring.

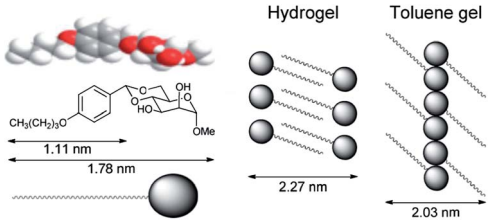

Fig. 9 The molecular length of **4** by CPK molecular modelling on the basis of PM3 calculation and the proposed molecular packing of **4** in hydrogel and toluene gel.

Thixotropic behaviour

Thixotropy is a phenomenon characteristically observed for LMWGs and has garnered considerable interest from gel scientists because of its significant relationship with some biological self-healing processes, such as those of muscular fibers and injured neural fibers, and with industrial applications, for materials such as cosmetics, paints, biomaterials and foodstuffs.[38–47] We examined this behaviour for derivatives **Bn**, **1–6** and **7** at their CGCs (Fig. 11 and 12). The toluene gels were permitted to rest for 1 h at RT after the mixtures of mannose derivatives were heated, and then shear stress was introduced *via* vortex mixing. After 1 h at RT, the sample vials were inverted. The samples prepared from **1–6** and **7** showed the regeneration of the gels, indicating that they possess thixotropic properties, whereas the sample prepared from **Bn** does not.

Furthermore, the thixotropic properties of several gels prepared from mannose derivatives **2** and **6** were examined in more detail (Fig. 13). For **2**, the gels of toluene, olive oil, IPM and ethylene glycol indicated thixotropic properties, whereas those of octane, cyclohexane and SH245 did not. Interestingly, the gels prepared from **6** exhibited thixotropic properties with octane, cyclohexane, toluene, SH245, olive oil, IPM and ethylene glycol. Thixotropic processes involve the self-assembly of small pieces of fibers to form bundled fibers.[44] These results reveal that the self-assembly process was induced by the van der Waals interactions between the alkoxy chains on the gelators. In particular, the van der Waals interactions between the alkoxy chains on gelator **6** (with the longest alkoxy chain among the

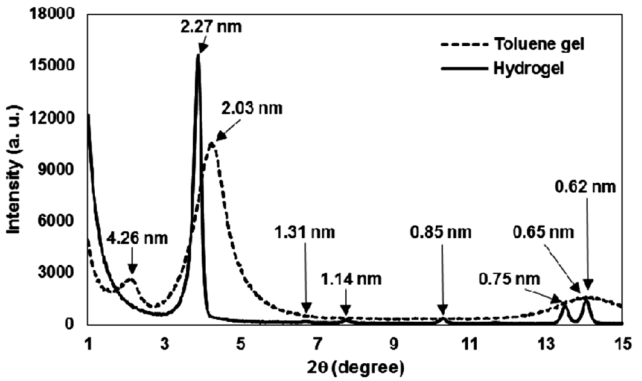

Fig. 8 XRD measurements of the xerogels of organogel (toluene) and hydrogel prepared from **2**.

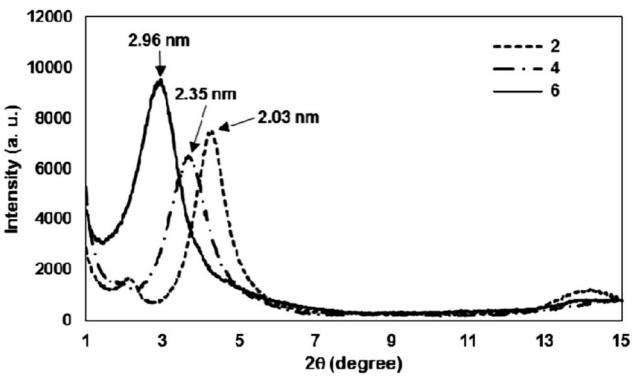

Fig. 10 XRD measurements of the xerogels prepared from toluene with **2**, **4** and **6**.

Fig. 11 Thixotropic behaviour of organogels prepared from **3** with toluene (left), after shear stress (middle) and after 1 h at RT (right).

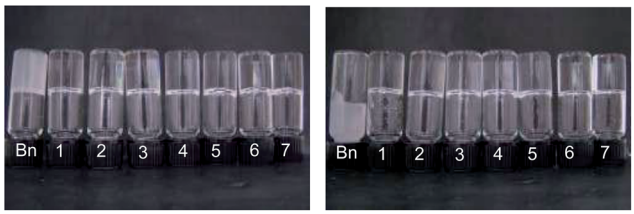

Fig. 12 Thixotropic behaviour of organogels prepared from **Bn** and **1**–**7** with toluene (left) and after applying shear stress, then resting for 1 h at RT (right).

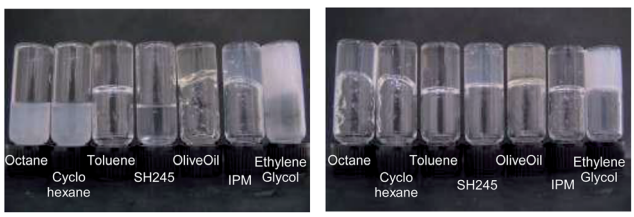

Fig. 13 Thixotropic behaviour of several gels formed from several solvents and **2** (left) or **6** (right).

mannose derivatives in this paper) are stronger than those of **2**. Therefore, **6** induced thixotropic properties in more of the gels formed from various solvents than **2**.

Conclusions

We demonstrated that mannose derivatives with various alkoxy substituents are able to gelate organic solvents and protic solvents. Through this study, we have established that as a general tendency, the mannose derivatives bearing a short linear alkoxy chain tend to gelate the nonpolar solvents such as toluene and cyclohexane at a low concentration. On the other hand, those bearing a long linear alkoxy chain tend to gelate polar and protic solvents (*e.g.*, ethylene glycol) at a low concentration. Furthermore, LMWGs **2** and **6** exhibited thixotropic properties with a wide range of solvent groups. It has thus become clear that the proper alkoxy chain at the *para* position of the aromatic ring imparts transparency, stability and thixotropic behavior to the gels. We are now extending our research toward the functional application of these gels possessing unique physical properties. In the future, we will report on the results obtained from these gels.

Experimental section

Apparatus for spectroscopic measurements

^{1}H and ^{13}C NMR spectra were acquired on a JEOL JNM-ECA 600 instrument. Chemical shifts were reported in ppm from tetramethylsilane for ^{1}H NMR spectra and $CDCl_3$ for ^{13}C NMR spectra as an internal standard. EI and FAB mass spectra were measured on a JEOL JMS-700 instrument.

Synthesis of methyl-4,6-*O*-(4-butoxybenzylidene)-α-D-mannopyranoside (2)

Copper(II) tetrafluoroborate (48 mg, 0.2 mmol) was added to a mixture of 4-butoxybenzaldehyde (3.6 g, 20 mmol) and trimethyl orthoformate (4.4 mL, 40 mmol) in anhydrous methanol (8 mL) under nitrogen atmosphere. The reaction mixture was stirred for 1 h at RT. After 1 h, the reaction mixture was quenched with saturated $NaHCO_3$ and extracted with ethyl acetate. The extracts were washed with brine, dried over Na_2SO_4, filtered and concentrated under reduced pressure. The obtained clear oil was afforded to the next reaction without further purification.

A solution of crude dimethylacetal in DMF (10 mL) was added dropwise to a suspension of methyl-α-D-mannopyranoside (4.3 g, 22 mmol) and *p*-toluenesulfonic acid (98 mg, 0.5 mmol) in anhydrous DMF (20 mL) under a nitrogen atmosphere. The reaction mixture was stirred for 10 min at RT and for 2 h under reduced pressure at RT. After 2 h, the reaction mixture was quenched with saturated $NaHCO_3$ and extracted with ethyl acetate. The extracts were washed with brine, dried over Na_2SO_4, filtered and concentrated under reduced pressure. The crude product was purified by column chromatography (SiO_2; hexane–ethyl acetate from 70/30 to 50/50, vol/vol). The desired product, **2**, was obtained as a white solid (3.2 g, 45%).

Methyl-4,6-*O*-(4-butoxybenzylidene)-α-D-mannopyranoside (2). δ_H (600 MHz, $CDCl_3$): 7.40 (2H, d, J = 8.5 Hz), 6.89 (2H, d, J = 8.8 Hz), 5.52 (1H, s), 4.77 (1H, s), 4.31–4.22 (1H, m), 4.10–4.02 (2H, m), 3.96 (2H, t, J = 6.6 Hz), 3.93–3.86 (1H, m), 3.85–3.76 (2H, m), 3.40 (3H, s), 2.66–2.60 (2H, br), 1.80–1.71 (2H, m), 1.53–1.43 (2H, m), 0.97 (3H, t, J = 7.6 Hz). δ_C (150 MHz, $CDCl_3$): 159.86, 129.46, 127.51, 114.32, 102.29, 101.21, 78.81, 70.82, 68.82, 68.73, 67.75, 62.89, 55.10, 31.23, 19.20, 13.82. HRMS (EI^+): m/z calcd for $C_{18}H_{26}O_7$ (M^+): 354.1679; found: 354.1682.

The other mannose derivatives are described in the ESI.†

Gelation tests of organic solvents, mixed solvents and water

The gelator and the solvent were put in a sealed-capped vial and heated in a dry bath until the solid was dissolved. The solution

was cooled at room temperature. If the stable gel was observed at this stage, it was classified with CGC values (wt%) in Table 1.

Gel–sol phase transition temperatures

A sealed vial containing the gel was immersed in a thermostatic dry bath. In 5 °C increments, the sample vial was inverted and T_{gel} was defined as the temperature at which gel–sol consistency was observed.

TEM observations

TEM imaging was performed on a JEOL JEM-2010HCKM instrument. The gel was prepared in a sample tube. For the TEM measurements, the samples were obtained by dipping a carbon-coated copper grid in the gel and dried under vacuum for more than 12 h. The dried grid was negatively stained with 1% phosphotungstic acid adjusted to pH 7 for 5 or 10 min. The grids were washed with water and dried under vacuum for more than 12 h. The TEM accelerating voltage was 200 kV.

SEM observations

FE-SEM imaging was performed on a Hitachi SU-8000 instrument at the Center of Advanced Instrumental Analysis, Kyushu University. The xerogel of **1** was obtained by freezing and pumping a gel of **1** for 5–14 h. The obtained xerogel was thus not coated with metal. The SEM accelerating voltage was less than 0.5 kV.

AFM observations

AFM was performed on an SII NanoTechnology Inc. Nanonavi/Nanocute instrument (now Hitachi High-Tech Science Corp.). For the AFM measurements, a droplet of the solution of **2** or **6** at 0.02 wt% in toluene was placed on highly ordered pyrolytic graphite (HOPG). After 1 h, the substrates were dried under vacuum for more than 12 h.

XRD measurements

Powder XRD patterns were measured on a Rigaku RINT-TTR III X-ray diffractometer equipped with CuKα radiation (50 kV, 300 mA) at a scanning rate of 1° min^{-1}.

Acknowledgements

We thank Dr Yumi Fukunaga for the support and valuable advice regarding TEM observations and Mr Taisuke Matsumoto for the support with XRD measurements. We thank Dr Osamu Hirata and Dr Akihiro Tanaka for their valuable comments and discussions.

References

1 P. Terech and R. G. Weiss, *Chem. Rev.*, 1997, **97**, 3133–3160.
2 O. Gronwald, E. Snip and S. Shinkai, *Curr. Opin. Colloid Interface Sci.*, 2002, **7**, 148–156.
3 L. A. Estroff and A. D. Hamilton, *Chem. Rev.*, 2004, **104**, 1201–1218.
4 N. M. Sangeetha and U. Maitra, *Chem. Soc. Rev.*, 2005, **34**, 821–836.
5 A. Ajayaghosh, V. K. Praveen and C. Vijayakumar, *Chem. Soc. Rev.*, 2008, **37**, 109–122.
6 A. R. Hirst, B. Escuder, J. F. Miravet and D. K. Smith, *Angew. Chem., Int. Ed.*, 2008, **47**, 8002–8018.
7 D. K. Smith, *Chem. Soc. Rev.*, 2009, **38**, 684–694.
8 M.-O. M. Piepenbrock, G. O. Lloyd, N. Clarke and J. W. Steed, *Chem. Rev.*, 2010, **110**, 1960–2004.
9 A. Dawn, T. Shiraki, S. Haraguchi, S. Tamaru and S. Shinkai, *Chem.–Asian. J.*, 2011, **6**, 266–282.
10 L. E. Buerkle and S. J. Rowan, *Chem. Soc. Rev.*, 2012, **41**, 6089–6102.
11 J. Raeburn, A. Z. Cardoso and D. J. Adams, *Chem. Soc. Rev.*, 2013, **42**, 5143–5156.
12 G. Yu, X. Yan, C. Han and F. Huang, *Chem. Soc. Rev.*, 2013, **42**, 6697–6722.
13 K. Yoza, Y. Ono, K. Yoshihara, T. Akao, H. Shinmori, M. Takeuchi, S. Shinkai and D. N. Reinhoudt, *Chem. Commun.*, 1998, 907–908.
14 J. Cui, A. Liu, Y. Guan, J. Zheng, Z. Shen and X. H. Wan, *Langmuir*, 2010, **26**, 3615–3622.
15 S. R. Jadhav, P. K. Vemula, R. Kumar, S. R. Raghavan and G. John, *Angew. Chem., Int. Ed.*, 2010, **49**, 7695–7698.
16 G. Wang, H. Yang, S. Cheuk and S. Coleman, *Beilstein J. Org. Chem.*, 2011, **7**, 234–242.
17 A. Vidyasagar, K. Handore and K. M. Sureshan, *Angew. Chem., Int. Ed.*, 2011, **50**, 8021–8024.
18 M. F. Abreu, V. T. Salvador, L. Vitorazi, C. E. N. Gatts, D. R. dos Santos, R. Giacomini, S. L. Cardoso and P. C. M. L. Miranda, *Carbohydr. Res.*, 2012, **353**, 69–78.
19 E. Bedini, L. Cirillo and M. Parrilli, *Tetrahedron*, 2013, **69**, 1285–1296.
20 K. Yoza, N. Amanokura, Y. Ono, T. Akao, H. Shinmori, M. Takeuchi, S. Shinkai and D. N. Reinhoudt, *Chem.–Eur. J.*, 1999, **5**, 2722–2729.
21 O. Gronwald, K. Sakurai, R. Luboradzki, T. Kimura and S. Shinkai, *Carbohydr. Res.*, 2001, **331**, 307–318.
22 O. Gronwald and S. Shinkai, *J. Chem. Soc., Perkin Trans. 2*, 2001, 1933–1937.
23 O. Gronwald and S. Shinkai, *Chem.–Eur. J.*, 2001, **7**, 4328–4334.
24 M. Mukai, H. Minamikawa, M. Aoyagi, T. Shimizu and M. Hogiso, *J. Colloid Interface Sci.*, 2000, **224**, 154–160.
25 J. H. Jung, G. John, M. Masuda, K. Yoshida, S. Shinkai and T. Shimizu, *Langmuir*, 2001, **17**, 7229–7232.
26 J. H. Jung, S. Shinkai and T. Shimizu, *Chem.–Eur. J.*, 2002, **8**, 2684–2690.
27 S. Kiyonaka, S. Shinkai and I. Hamachi, *Chem.–Eur. J.*, 2003, **9**, 976–983.
28 M. Suzuki, M. Yumoto, M. Kimura, H. Shirai and K. Hanabusa, *Helv. Chim. Acta*, 2004, **87**, 1–10.
29 M. Suzuki, S. Owa, M. Kimura, A. Kurose, H. Shirai and K. Hanabusa, *Tetrahedron Lett.*, 2005, **46**, 303–306.
30 M. Suzuki, M. Nanbu, M. Yumoto, H. Shirai and K. Hanabusa, *New J. Chem.*, 2005, **29**, 1439–1444.

31 M. Suzuki, T. Sato, H. Shirai and K. Hanabusa, *New J. Chem.*, 2007, **31**, 69–74.
32 S. Kiyonaka, S. Shinkai and I. Hamachi, *Chem.–Eur. J.*, 2003, **9**, 976–983.
33 Y. Imura, K. Matsue, H. Sugimoto, R. Ito, T. Kondo and T. Kawai, *Chem. Lett.*, 2009, **38**, 778–779.
34 T. Kar, S. Debnath, D. Das, A. Shome and P. K. Das, *Langmuir*, 2009, **25**, 8639–8648.
35 N. Yan, G. He, H. Zhang, L. Ding and Y. Fang, *Langmuir*, 2010, **26**, 5909–5917.
36 N. Minakuchi, K. Hoe, D. Yamaki, S. Ten-no, K. Nakashima, M. Goto, M. Mizuhata and T. Maruyama, *Langmuir*, 2012, **28**, 9259–9266.
37 R. Wakabayashi, T. Ikeda, Y. Kubo, S. Shinkai and M. Takeuchi, *Angew. Chem., Int. Ed.*, 2009, **48**, 6667–6670.
38 D. M. Blow and A. Rich, *J. Am. Chem. Soc.*, 1960, **82**, 3566–3571.
39 J. Brinksma, B. L. Feringa, R. M. Kellog, R. Vreeker and J. van Esch, *Langmuir*, 2000, **16**, 9249–9255.
40 M. Lescanne, P. Grondin, A. d'Aleo, F. Fages, J.-L. Pozzo, O. M. Monval, P. Reinheimer and A. Colin, *Langmuir*, 2004, **20**, 3032–3041.
41 M. Shirakawa, N. Fujita and S. Shinkai, *J. Am. Chem. Soc.*, 2005, **127**, 4164–4165.
42 T. Shirosaki, S. Chowdhury, M. Takafuji, D. Alekperov, G. Popova, H. Hachisako and H. Ihara, *J. Mater. Res.*, 2006, **21**, 1274–1278.
43 X. Huang, S. R. Raghavan, P. Terech and R. G. Weiss, *J. Am. Chem. Soc.*, 2006, **128**, 15341–15352.
44 P. Mukhopadhyay, N. Fujita, A. Takada, T. Kishida, M. Shirakawa and S. Shinkai, *Angew. Chem., Int. Ed.*, 2010, **49**, 6338–6342.
45 A. Shundo, K. Mizuguchi, M. Miyamoto, M. Goto and K. Tanaka, *Chem. Commun.*, 2011, **47**, 8844–8846.
46 X. Hou, D. Gao, J. Yan, Y. Ma, K. Liu and Y. Fang, *Langmuir*, 2011, **27**, 12156–12163.
47 H. Hoshizawa, Y. Minemura, K. Yoshikawa, M. Suzuki and K. Hanabusa, *Langmuir*, 2013, **29**, 14666–14673.